

## Supplementary Information

### Phosphine-Oxide Modulator Ameliorates Hole Injection for Blue Perovskite Light-Emitting Diodes

Xiangyang Fan,<sup>a</sup> Yu Wang,<sup>b</sup> Xinyu Shen,<sup>\*c,d</sup> Zhongkai Yu,<sup>c</sup> Woo Hyeon Jeong,<sup>c</sup> Ji Won Jang,<sup>c</sup> Yeong Gyeong Kim,<sup>a</sup> Seung-Je Woo,<sup>f</sup> Hyungju Ahn,<sup>g</sup> Tae-Woo Lee,<sup>f</sup> Hyosung Choi,<sup>e</sup> Sung Heum Park,<sup>a</sup> Feng Gao,<sup>b</sup> and Bo Ram Lee <sup>\*c</sup>

<sup>a</sup> Department of Physics , Pukyong National University, and CECS Research Institute, Core Research Institute, Busan 48513, Republic of Korea

<sup>b</sup> Biomolecular and organic electronics, Department of Physics, Chemistry and Biology (IFM), Linköping University, Linköping SE-58183, Sweden

<sup>c</sup> School of Advanced Materials Science and Engineering, Sungkyunkwan University (SKKU), Suwon, 16419 Republic of Korea  
E-mail: shenxinyu93@gmail.com (X.S), brlee@skku.edu (B. R. L.)

<sup>d</sup> Clarendon Laboratory, Department of Physics, University of Oxford, Oxford, UK

<sup>e</sup> Department of Chemistry, Research Institute for Convergence of Basic Science, Research Institute for Natural Sciences, Hanyang University, Seoul 04763, Republic of Korea

<sup>f</sup> Department of Materials Science and Engineering, Seoul National University, Seoul 08826, Republic of Korea

<sup>g</sup> Pohang Accelerator Laboratory, POSTECH, Pohang 37673, Republic of Korea

## Contents:

1. Experimental
  - 1.1 Materials
  - 1.2 Synthesis of TMFPPO
  - 1.3 Preparation perovskite precursor and blended HTLs
  - 1.4 Simulation Methods
  - 1.5 Fabrications of PeLEDs
  - 1.6 Characterization
2. Fig. S1: J-V curve of hole-only device based on different HTLs.
3. Fig. S2: UV-vis absorption spectra of various blended HTLs.
4. Fig. S3: AFM images and contact angle measurements of TMFPPO film.
5. Fig. S4: XRD of the quasi-2D perovskite film deposited on various HTLs.
6. Fig. S5: Hole distribution for the devices with PVK and PVK:TMFPPO (9:1) at 4V bias.
7. Table S1: Hole Mobility of different HTLs.
8. Table S2: Optical band gap of different blended HTLs.
9. Table S3: Time-resolved PL decay profiles of perovskite with various HTL films.
10. Table S4: Operational stability of PeLEDs.
11. Table S5: Summary of quasi-2D blue (~ 480 nm) PeLEDs.
12. Table S6: Parameters used for Simulations.

## 1. Experimental section

### 1.1 Materials

Poly(3,4-ethylenedioxythiophene): poly-styrene sulfonate (PEDOT:PSS, Clevios AI 4083) was purchased from Heraeus Clevios, Indium tin oxide-based transparent conductive electrode (~4.5  $\Omega$ /sq ITO) was purchased from AMG. poly (9-vinylcarbazole) (PVK,  $M_w=1, 100,000$  g mol<sup>-1</sup>), yttrium (III) chloride (YCl<sub>3</sub>, 99.99%), 2-phenylethylamine hydrochloride (PEACl,  $\geq 98\%$ ), cesium bromide (CsBr, 99.999%), lead bromide (PbBr<sub>2</sub>,  $\geq 98\%$ ), chlorobenzene (CB, 99.8%) dimethyl sulfoxide (DMSO, 99.9%) and chloroform (CF,  $\geq 99\%$ ) were purchased from Sigma Aldrich. Hydrogen peroxide (H<sub>2</sub>O<sub>2</sub>, 27%) was purchased from Thermo Fisher, lithium fluoride (LiF, 99.9%) was obtained from iTASCO. And 2,2',2''-(1,3,5-benzinetriyl) tris(1-phenyl-1-H-benzimidazole) (TPBi, 99.9%) was purchased from OSM.

### 1.2 Synthesis of TMFPPO

Tris(4-trifluoromethylphenyl)phosphine (TMFP, M.W. 466.28) 0.295g, 0.633mmol. Stir in a bottle to dissolve 1mL of Chloroform (CF, m.w. 119.38). When completely dissolved, add 1.15mL of 27% H<sub>2</sub>O<sub>2</sub> solution and mix. After thorough stirring overnight, the obtained mixture solution was extracted by chloroform. The supernatant was poured away, and the remaining suspension was dried overnight in an incubator to obtain the white powder - Tris(4-trifluoromethylphenyl)phosphine-oxide (TMFPPO).

### 1.3 Preparation perovskite precursor and blended HTLs

Perovskite: 91.75 mg PbBr<sub>2</sub> and 53.2 mg CsBr were dissolved in 1 mL DMSO, PEACl was dissolved in DMSO with a concentration of 1.2M and YCl<sub>3</sub> was dissolved in DMSO with a concentration of 0.25M. Then, 125  $\mu$ L PEACl solution and 10  $\mu$ L YCl<sub>3</sub> solution were added into the 0.5 mL CsPbBr<sub>3</sub> precursor solution. The as-prepared was stirred at 50 °C and can be

used after filtering with a 0.2  $\mu\text{m}$  hydrophilic filter.

Blended HTLs: Dissolving PVK and TMFPPO with different weight ratios (10:0, 9:1, 7:3) in CB with the concentration of 4 mg mL<sup>-1</sup>). The solution was spin-coated on PEDOT:PSS film at 4000 rpm for 40 s and the substrates were annealed at 120 °C for 10 minutes.

#### ***1.4 Simulation Methods***

Device Simulations were conducted using the COMSOL Multiphysics platform, specifically employing the semiconductor module. COMSOL serves as a robust platform for the numerical simulation of partial differential equations (PDEs). In this work, we utilized drift-diffusion equations to gain a deeper understanding of the underlying device physics. Mobilities were considered to be independent of the electric field, as these can be directly determined from SCLC measurements. To accurately represent the recombination process within the device, we applied the ABC model and the recombination profiles in the manuscript were also calculated based on ABC model.

#### ***1.5 Devices fabrication***

ITO-coated glass substrates were cleaned by an ultra-sonification process in deionized water, acetone and isopropanol for 30 min. Poly(3,4-ethylenedioxythiophene):poly(styrenesulfonate) (PEDOT:PSS, AI 4083, Clevios) solution (filtered through a 0.45  $\mu\text{m}$  CA filter) was spin-coated at 4000 rpm for 45 s onto the ITO substrate then annealed at 150 °C for 10 min. poly(9-vinylcarbazole) (PVK,  $M_w=1,100,000 \text{ g mol}^{-1}$ ) solution dissolved in chlorobenzene (0.7 wt%) was spin-coated at 4000 rpm for 45 s onto PEDOT:PSS for the emissive layer. The perovskite precursor solution was spin-coated on HTL films at 500 rpm for 5 s and 5000 rpm for 40 s. After 15 s of spin-coating at 5000 rpm, 300  $\mu\text{L}$  CB was dropped onto the substrate

with above layers. After annealing at 100°C for 2.5 minutes, the samples were transferred to the thermal evaporation chamber, and TPBi (40 nm), LiF (1 nm) and Al (100 nm) were sequentially deposited at about  $1 \times 10^{-6}$  Torr by the thermal evaporation method. According to the area covered by the aluminum electrode, the defined area of the unit device is 0.135 cm<sup>2</sup>.

## ***1.6 Characterization***

Device Simulations were conducted using the COMSOL Multiphysics platform, specifically employing the semiconductor module. COMSOL serves as a robust platform for the numerical simulation of partial differential equations (PDEs). In this work, we utilized drift-diffusion equations to gain a deeper understanding of the underlying device physics. Mobilities were thought independent of the electric field, as these can be directly determined from SCLC measurements. To accurately represent the recombination process within the device, we applied the ABC model and the recombination profiles in the manuscript were also calculated based on ABC model. AFM was measured by a scanning probe microscope (Icon-PT-PLUS, RUKER). SEM was measured with Field Emission Scanning Electron Microscope-Schottky type (MIRA3 LMH, TESCAN). Steady-state PL measurements were carried out using a pulsed xenon lamp. Time-resolved PL decay measurements were carried out by a He-Cd laser operating at a wavelength of 370 nm. The J–V–L characteristics, EQE and EL spectra were measured using a Konica Minolta spectroradiometer (CS-2000) with a Keithley 2400 source meter. Device characteristics were measured under ambient air conditions with encapsulation. UPS spectra were collected using a photoelectron spectrometer (Thermo Fisher Scientific Theta Probe) with a He I (21.22 eV) ultraviolet source in Smart Lab at the Hanyang LINC + analytical equipment center (Seoul). UV-Vis absorption spectra were measured by Varian Cary 5000 spectrophotometer. XRD patterns were measured using a using an X’Pert-MPD diffractometer (Philips, Netherlands) employing CuK $\alpha$  radiation. FTIR were measured with

Fourier Transform Infra-Red Spectrometer (FT-4100, JASCO). The GIWAXS results were observed using Xrays ( $\alpha_i = 0.12$  deg ,  $E = 19.8805$  keV)

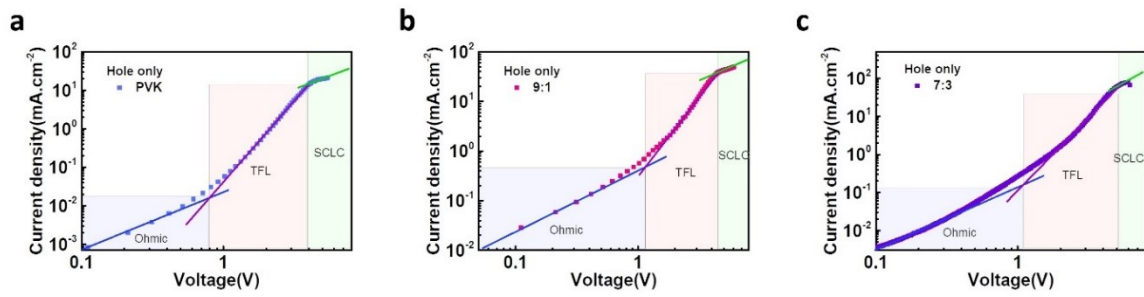


**Fig. S1.** J-V curve of hole-only device based on different HTLs.

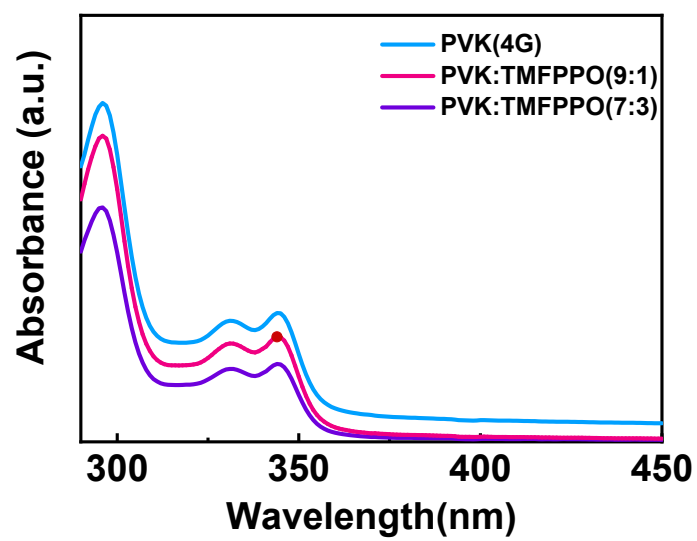


**Fig. S2.** UV-vis absorption spectra of various blended HTLs.

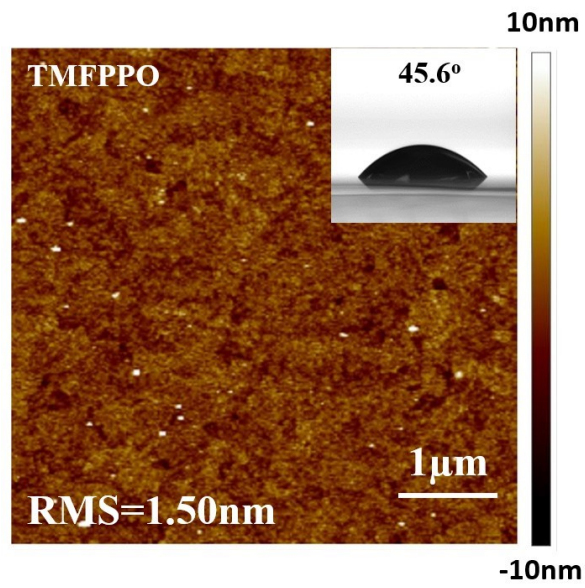


**Fig. S3.** AFM images and contact angle of TMFPPO film

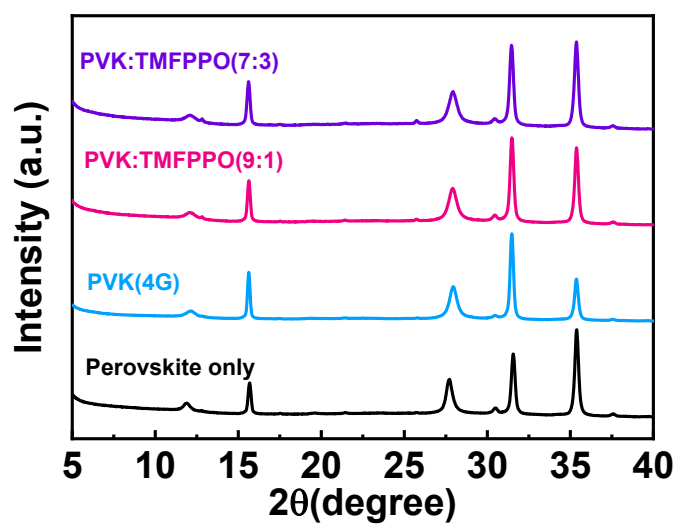


**Fig. S4.** XRD of the quasi-2D perovskite film deposited on various HTLs.

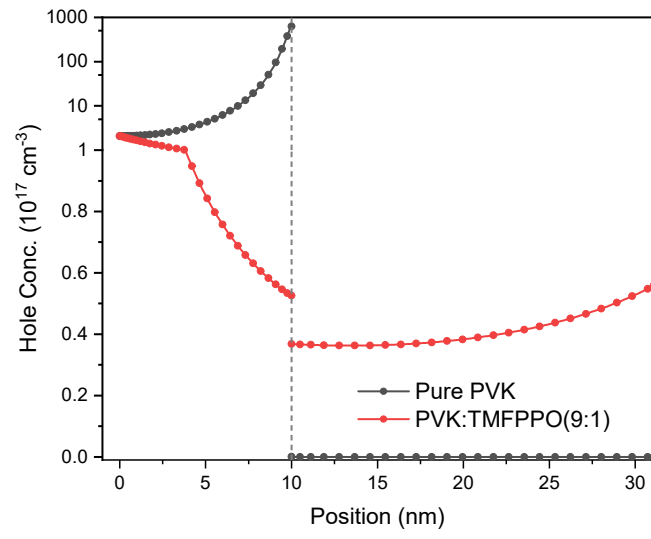


**Fig. S5.** Hole distribution for the devices with PVK and PVK:TMFPPO (9:1) at 4V bias.

**Table S1.** Hole Mobility of different HTLs.

HTLs	Hole Mobility [ $\text{cm}^2/(\text{V}\cdot\text{s})$ ]
PVK	$1.04 \times 10^{-5}$
PVK:TMFPPO(9:1)	$1.84 \times 10^{-5}$
PVK:TMFPPO(7:3)	$2.73 \times 10^{-5}$
TMFPPO	$1.26 \times 10^{-4}$

**Table S2.** Optical band gap of different blended HTLs.

	$E_{gap}^{opt}$ (eV)	$\lambda_{edge}$ (nm)
PVK	3.52	352
PVK:TMFPPO (9:1)	3.52	352
PVK:TMFPPO (7:3)	3.52	352

**Table S3.** Time-resolved PL decay profiles of perovskite with various HTL films.

Sample configuration	$\tau_1$ (ns)	$A_1$ (%)	$\tau_2$ (ns)	$A_2$ (%)	$\tau_3$ (ns)	$A_3$ (%)	$\tau_{\text{avg}}$ (ns)
Perovskite	11.02	41.38	2.36	48.66	63.57	7.76	34.45
PVK	0.72	43.33	5.12	37.70	32.65	8.48	20.05
PVK:TMFPPO (9:1)	2.55	58.45	9.32	0.38	46.60	4.37	18.64
PVK:TMFPPO (7:3)	2.62	61.54	9.73	0.36	47.90	4.07	18.59

$\tau_1, \tau_2,$  and  $\tau_3$ : Lifetimes       $A_1, A_2$  and  $A_3$ : Respective fractional contributions

$\tau_{\text{avg}}$ : Average lifetime ( $\tau_{\text{avg}}$ ) which is calculated using  $\tau_{\text{avg}} = \sum_{i=1}^3 A_i \cdot \tau_i$

**Table S4.** Operational stability of PeLEDs.

<b>Sample configuration</b>	<b>T<sub>50</sub> (s)</b>
PVK	117
PVK:TMFPPO (9:1)	126
PVK:TMFPPO (7:3)	99

**Table S5.** Summary of quasi-2D blue (~ 480 nm) PeLEDs.

Perovskite	Emission peak [nm]	EQE <sub>max</sub> [%]	L <sub>max</sub> [cd/m <sup>2</sup> ]	CE <sub>max</sub> [cd/A]	T <sub>50</sub>	Reference
<sup>1</sup> PEA <sub>2</sub> Cs <sub>1.6</sub> MA <sub>0.4</sub> Pb <sub>3</sub> Br <sub>10</sub>	479	5.2	468	-	90min@100cd/m <sup>2</sup>	J. Am. Chem. Soc. <b>2020</b> 142, 5126
<sup>2</sup> MePEABr:CsPbBr <sub>3</sub>	477	2.9	154	2.6	9s@70cd/m <sup>2</sup>	Adv. Funct. Mater. <b>2021</b> 31, 2103299
<sup>1</sup> PEA-Rb <sub>0.3</sub> Cs <sub>0.7</sub> PbBr <sub>2.7</sub> Cl <sub>0.3</sub>	475	10.1	14000	-	100s@100cd/m <sup>2</sup>	Adv. Mater. <b>2021</b> 33, 2100783
<sup>3</sup> NEA-FAPbBr <sub>3-x</sub> Cl <sub>x</sub>	474	3.1	2810	-	75s@1000cd/m <sup>2</sup>	Nano Energy <b>2021</b> 79, 105486
<sup>4</sup> (Cs/FA/p-F-PEA)Pb(Cl/Br) <sub>3</sub>	469	4.14	451	2.71	14min@1mA/cm <sup>2</sup>	Adv. Funct. Mater. <b>2020</b> 2006736
<sup>5</sup> (Rb/Cs/FA)Pb(Cl/Br) <sub>3</sub> :TTDDA	467	5.5	200~	-	87s@5mA/cm <sup>2</sup>	Nat. Commun. <b>2021</b> 12, 361
<sup>1</sup> CsPbBr <sub>3</sub> :PEACl:YCl <sub>3</sub>	478	5.30	167	4.42	112s@30cd/m <sup>2</sup>	JMCA. <b>2022</b> 10, 13928
<sup>1</sup> PEABr:CsPbBr <sub>3</sub>	490	11.5	102	-	41min@33cd/m <sup>2</sup>	Nano-Micro Letters. <b>2022</b> 2, 23
<sup>6</sup> PABr:PEABr:CsPbBr <sub>3-x</sub> Cl <sub>x</sub>	480	10.98	548	-	7.6min@1.5mA/cm <sup>2</sup>	ACS Energy Lett. <b>2022</b> , 7, 10
<sup>7</sup> FAOAc:CsPbBr <sub>3-x</sub> Cl <sub>x</sub>	477	8.8	1361	7.6	120s@100cd/m <sup>2</sup>	Adv. Funct. Mater. <b>2022</b> 32, 2105164
<sup>8</sup> PBABr: CsPbBr <sub>3</sub>	471	2.9	100	-	105s@10cd/m <sup>2</sup>	Adv. Optical Mater. <b>2023</b> , 11, 2202029
<sup>9</sup> BDABr <sub>2</sub> : PEABr: CsPbBr <sub>3</sub>	487	3.82	442	-	77s@30cd/m <sup>2</sup>	Chem. Commun., <b>2023</b> , 59,5906
<sup>1</sup> CsPbBr <sub>3</sub> :PEACl:YCl <sub>3</sub>	477	7.23	136	6.96	126s@30cd/m <sup>2</sup>	<b>Our work</b>

<sup>1</sup>PEA: phenylethylammonium, <sup>2</sup>MePEA: methoxy phenethylammonium, <sup>3</sup>NEA: 2-(2-naphthyl)ethanamine, <sup>4</sup>p-F-PEA: 4-Fluorophenylethylammonium, <sup>5</sup>TTDDA: 4,7,10-trioxa-1,13-tridecanediamin, <sup>6</sup>PABr:propylamine, <sup>7</sup>FAOAc:formami-dine acetate, <sup>8</sup>PBABr: 4-phenylbutylammonium, <sup>9</sup>BDA: 1,4-butanediamonium.

	Perovskite	TPBi	PVK	PVK:TMFPPO (9:1)
Ec(eV)	3.55 <sup>1</sup>	2.8	2.31	2.68
Ev(eV)	6.15 <sup>1</sup>	6.2	5.83	6.19
Mobility(cm <sup>2</sup> /V/s)	2×10 <sup>-32,3</sup>	1.0×10 <sup>-5</sup>	1.04×10 <sup>-5</sup>	1.84×10 <sup>-5</sup>
Relative Permittivity	10 <sup>4,5</sup>	3	3	3
Work Function (eV)	3.84 <sup>6,7</sup>	3.16	4.66	4.84
SRH Coefficient (s <sup>-1</sup> )	1×10 <sup>-7</sup>			
Radiative Coefficient (cm <sup>3</sup> s <sup>-1</sup> )	1×10 <sup>-9</sup>			
Auger Coefficient (cm <sup>6</sup> s <sup>-1</sup> )	1×10 <sup>-28</sup>			

**Table S6.** Parameters used for Simulations.

## References

1. G. S. Kumar, R. R. Sumukam and B. Murali, *J. Mater. Chem. C*, 2020, **8**, 14334-14347.
2. X. Lai, W. Li, X. Gu, H. Chen, Y. Zhang, G. Li, R. Zhang, D. Fan, F. He and N. J. Zheng, *Chemical Engineering Journal* 2022, **427**, 130949.
3. N. K. Tailor, R. Ranjan, S. Ranjan, T. Sharma, A. Singh, A. Garg, K. S. Nalwa, R. K. Gupta and S. J. Satapathi, *J. Mater. Chem. A*, 2021, **9**, 21551-21575.
4. Z. Ren, J. Yu, Z. Qin, J. Wang, J. Sun, C. C. Chan, S. Ding, K. Wang, R. Chen and K. S. J. Wong, *Adv. Mater.*, 2021, **33**, 2005570.
5. Z. Ren, J. Sun, J. Yu, X. Xiao, Z. Wang, R. Zhang, K. Wang, R. Chen, Y. Chen and W. C. J. Choy, *Nano-Micro Lett.*, 2022, **14**, 66.
6. A. Zunger and O. I. Malyi, *Chemical Reviews*, 2021, **121**, 3031-3060.
7. F. Peña-Camargo, J. Thiesbrummel, H. Hempel, A. Musiienko, V. M. Le Corre, J. Diekmann, J. Warby, T. Unold, F. Lang, D. Neher and M. Stolterfoht, *Applied Physics Reviews*, 2022, **9**.